Journal of Power Sources 196 (2011) 4604–4608

Contents lists available at ScienceDirect

Journal of Power Sources

journal homepage: www.elsevier.com/locate/jpowsour

Short communication

Hydrogen desorption properties of MgH_2–$TiCr_{1.2}Fe_{0.6}$ nanocomposite prepared by high-energy mechanical alloying

Nafiseh Mahmoudi [a], A. Kaflou [b], A. Simchi [a,c,*]

[a] Department of Materials Science and Engineering, Sharif University of Technology, P.O. Box 11365-9466, Azadi Avenue, 14588 Tehran, Iran
[b] Institute for Advanced Materials and Renewable Energy, Iranian Research Organization for Science and Technology, P.O. Box 13135-115, Tehran, Iran
[c] Institute for Nanoscience and Nanotechnology, Sharif University of Technology, P.O. Box 11365-9466, Azadi Avenue, 14588 Tehran, Iran

ARTICLE INFO

Article history:
Received 15 May 2010
Received in revised form
19 December 2010
Accepted 3 January 2011
Available online 12 January 2011

Keywords:
Hydrogen storage materials
Magnesium hydride
Mechanical alloying
Nanostructures
Ti–Cr–Fe alloy

ABSTRACT

In the present work, high-energy mechanical alloying (MA) was employed to synthesize a nanostructured magnesium-based composite for hydrogen storage. The preparation of the composite material with composition of MgH_2–5 at% ($TiCr_{1.2}Fe_{0.6}$) was performed by co-milling of commercial available MgH_2 powder with the body-centered cubic (bcc) alloy either in the form of Ti–Cr–Fe powder mixture with the proper mass fraction (sample A) or prealloyed $TiCr_{1.2}Fe_{0.6}$ powder (sample B). The prealloyed powder with an average crystallite size of 14 nm and particle size of 384 nm was prepared by the mechanical alloying process. It is shown that the addition of the Ti-based bcc alloy to magnesium hydride yields a finer particle size and grain structure after mechanical alloying. As a result, the desorption temperature of mechanically activated MgH_2 for 4 h decreased from 327 °C to 262 °C for sample A and 241 °C for sample B. A high dehydrogenation capacity (~5 wt%) at 300 °C is also obtained. The effect of the Ti-based alloy on improvement of the dehydrogenation is discussed.

1. Introduction

Metal hydrides are promising candidates for hydrogen storage and so far many of them have been developed for practical use [1–3]. Among various metals, magnesium with its high theoretical hydrogen absorption capacity (7.6 wt%) and low cost has attracted considerable attention during the last decade for on board services. Many studies have been performed to improve the hydrogen absorption/desorption characteristics of MgH_2 in order to prepare an appropriate material for practical purposes at low temperatures [4]. Mechanical alloying of magnesium [5–10] and magnesium hydride [11–13] have been used to increase the surface to bulk ratio, induce stresses and defects in the structures, and refine the grain structure to improve the H-kinetics. Many researchers have also examined mechanical milling of MgH_2 with transition metals [14–17], intermetallic compounds [9,12,18,19], metal oxides [14,20], and graphite [21,22]. Recently, it has been reported that Ti-based bcc alloys exhibit a remarkable hydrogen storage capacity at room temperature [6,23–26]. Nevertheless, the slow reaction of Ti alloys with hydrogen causes no clear absorption–desorption plateau [27]. Yu et al. [28] used melt quenching technique together with alloy modification through vanadium, manganese, chromium, and iron addition to improve the hydrogen storage properties of bcc Ti-alloys. It was shown [27–31] that addition of a proper amount of these alloying elements and controlling of the cooling rate during quenching can improve the hydrogen capacity and absorption/desorption plateau pressure. Nevertheless, the cost of titanium alloys and the ease of oxidation limit their applications. Khrussanova et al. [9] prepared a Mg–Ti–V–Fe nanocomposite by mechanical alloying and showed that a high hydrogen absorption capacity (6.2 wt%) can be obtained at 350 °C, which is a significantly lower temperature than for pure magnesium. Liu et al. [6] prepared a Mg–Ti–Cr–V composite by mechanical alloying and reported 4 wt% hydrogen adsorption at 275 °C in 10 min. Besides these achievements, the obtained hydrogen kinetics still falls short of the requirements of the US Department of Energy for onboard hydrogen storage [32]; hence, further research is required to improve the H-kinetics of magnesium and magnesium hydride. The aim of this work is to study the effect of Ti–Cr–Fe addition on the desorption characteristics of MgH_2-based composite obtained by high-energy mechanical alloying. Titanium forms binary hydrides with a varying stoichiometry that may pump hydrogen to the magnesium surface [9]. On the other hand, iron and chromium influence the H-kinetics through active sites on the particles surfaces (catalytic effect). Therefore, the simultaneous effects of these elements on desorption properties of MgH_2 is worth investigating. In this work,

* Corresponding author at: Department of Materials Science and Enginering, Sharif University of Technology, P.O. Box 11365-9466, Azadi Avenue, Tehran 14588, Iran. Tel.: +98 21 6616 5261; fax: +98 21 6616 5262.
E-mail address: simchi@sharif.edu (A. Simchi).

0378-7753/$ – see front matter © 2011 Elsevier B.V. All rights reserved.
doi:10.1016/j.jpowsour.2011.01.001

these metals in the form of elemental powders or prealloyed powder were added to the magnesium hydride and the mixture was mechanically milled for different times. The effect of the alloying method on the dehydrogenation was studied and compared with pure magnesium hydride.

2. Experimental procedure

Commercial MgH_2 powder (98%, <105 μm) with an average particle size of 51 μm was purchased from Alfa Aesar, US. Ti (98%, <150 μm), Cr (95%, <100 μm), and Fe (98%, <150 μm) powders were supplied by Merck, Germany. MgH_2 with and without additives (Ti, Cr, and Fe) was milled in a SPEX 8000M shaker/miller under a high-purity argon atmosphere for various times. Stainless steel vial and balls (10 mm diameter) at the ball to powder weight ratio of 10:1 were used. Weighting, filling, and handling of the powders were performed in a glove box under the argon atmosphere. The following three sets of experiments were carried out:

(i) Mechanical milling of MgH_2 powder without the additives was performed for various times and the characteristics of powder particles were examined as the reference base.
(ii) A proper mixture of Ti, Cr and Fe powders was mechanically milled to process prealloyed $TiCr_{1.2}Fe_{0.6}$ (at%) powder with nanoscale grain size.
(iii) Mechanical alloying of MgH_2–5 at% ($TiCr_{1.2}Fe_{0.6}$) was performed by two different routes using elemental powders of Ti, Cr, and Fe with the proper mass fraction (sample A) or prealloyed $TiCr_{1.2}Fe_{0.6}$ powder (sample B). The effect of MA time on the desorption properties of the composite powders was studied.

The morphological changes of powder particles upon mechanical alloying were studied by scanning electron microscopy (SEM, Philips XL30). The size distribution of the particles was determined by a laser diffraction particle size analyzer (PSA, Malvem, UK). The particle size at n% of the cumulative curve, e.g. D_{10}, D_{50}, and D_{90}, was found out. The dehydrogenation behavior was studied by a simultaneous thermal analyzer (Netzsch STA 409) at a constant heating rate of 5 °C min^{-1} under a high purity argon atmosphere. X-ray diffraction (XRD) was performed by using Cu-K_α radiation on a Philips X'pert powder diffractometer. The crystallite size and lattice strain of MgH_2 (β) phase and the Ti-based alloy were estimated from the broadening of XRD peaks using Williamson–Hall method [14] according to the following equation:

$$\beta = 2\varepsilon \tan\theta + \frac{\lambda}{d\cos\theta} \quad (1)$$

where β is the peak broadening in the full width half maximum of θ degree, λ the X-ray wavelength, d the crystallite size, and ε is the lattice strain. The instrumental broadening was corrected by:

$$\beta^2 = \beta_{meas}^2 - \beta_{Inst}^2 \quad (2)$$

where β_{meas} and $\beta_{Inst.}$ are the measured and instrumental peak broadening, respectively.

3. Results

Fig. 1a shows XRD patterns of the Ti–Cr–Fe powder mixture after mechanical alloying for 2, 4, and 6 h. The XRD peak of the mixed Ti–Cr–Fe powder was included in the graph to compare the changes occurred during MA. The formation of the bcc phase after 2 h mechanical alloying was observed. Continuation of the mechanical alloying process resulted in the peak line broadening of the bcc alloy while disappearance of the titanium characteristic peaks revealed progressive homogenization of the powder

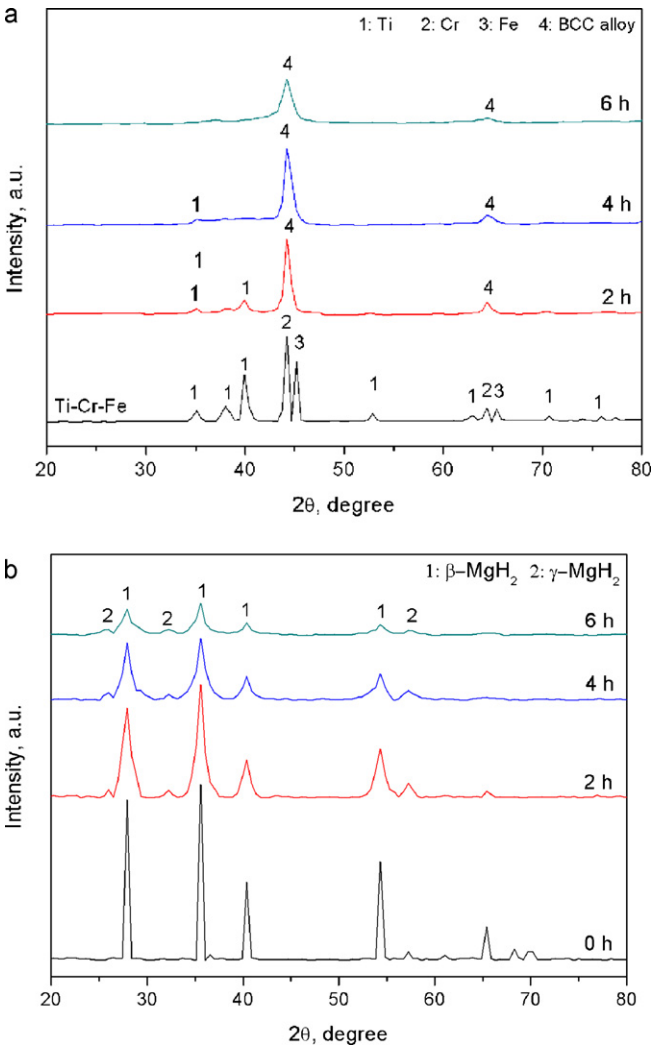

Fig. 1. XRD pattern of (a) Ti–Cr–Fe powder mixture, and (b) pure MgH_2 at some selected milling times. The pattern of mixed Ti–Cr–Fe powder is included in (a) to show the changes occurred during MA.

mixture. Fig. 1b shows the XRD patterns of pure MgH_2 powder at the selected milling times. The characteristic peaks of γ-MgH_2 phase were detected while the peaks of β-MgH_2 became broadened due to the high-energy impact of the milling balls. Table 1 reports the variation of average particle size, crystallite size, and lattice strain of the Ti–Cr–Fe and pure MgH_2 powders. A significant grain refinement occurred in both materials to attain nanostructured magnesium hydride and the Ti–Cr–Fe alloy with an average crystallite size of 16 and 14 nm, respectively. In spite of MgH_2, which the average particle size decreased from 51 μm to 27 μm,

Table 1
Particle size (D), crystallite size (d), lattice strain (ε) of magnesium hydride and the bcc-phase alloy at different milling times. D_n indicates the particle size at n% of the cumulative size distribution curve.

Powder	Time (h)	D_{50} (μm)	D_{90}–D_{10} (μm)	d (nm)	ε (%)
MgH_2	0	51	70	30	0
	2	25	286	23	0.7
	4	35	439	25	0.8
	6	27	199	16	0.6
Ti–Cr–Fe	2	0.62	662	69	–
	4	0.51	509	21	–
	6	0.38	384	14	0.6

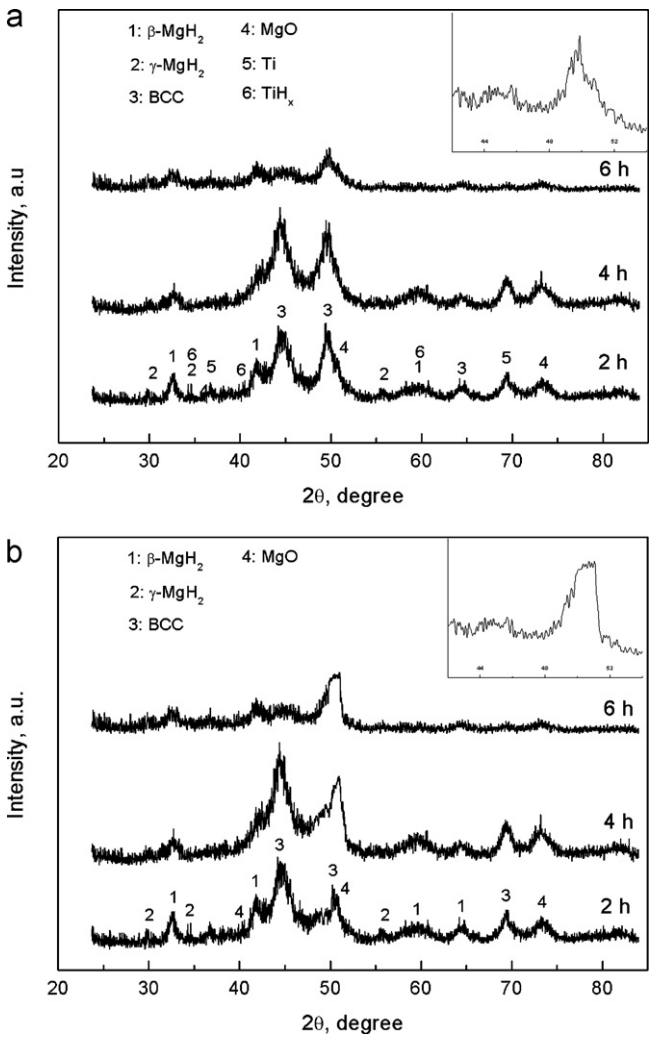

Fig. 2. XRD patterns of MgH_2–5 at% ($TiCr_{1.2}Fe_{0.6}$) nanocomposite at different milling times: (a) prepared by co-milling of MgH_2 and elemental powders of the transition metals, (b) synthesized by co-milling of MgH_2 and prealloyed $TiCr_{1.2}Fe_{0.6}$ alloy. The insert figures exhibit the main peaks of the milled powders for 6 h.

noticeable refinement in the particle size of the Ti-based alloy was attained.

Fig. 2a shows the XRD patterns of MgH_2–5 at% ($TiCr_{1.2}Fe_{0.6}$) alloy obtained by mechanical alloying of the magnesium hydride with the elemental powders of the transition metals (sample A). Although the main characteristic peaks of the constituents overlap, it can be seen that: (i) β- and γ-MgH_2 phases were detected at the three different milling times; (ii) oxidation of magnesium and formation of titanium hydride were noticeable; (iii) mechanical alloying under the above conditions did not lead to the formation of intermetallic phases in the system. The phase formation in the Ti–Cr–Fe system in Fig. 2a was found to be comparable with those of elemental powders (Fig. 1a); the major difference was the formation of titanium hydride. Fig. 2b shows the XRD patterns of MgH_2–5 at% ($TiCr_{1.2}Fe_{0.6}$) nanocomposite obtained by 6 h mechanical alloying of the magnesium hydride with the prealloyed Ti-based bcc alloy (sample B). The XRD pattern is rather similar to that of the elemental powder (Fig. 2a) except that titanium hydride was not formed. Table 2 reports the characteristics of the synthesized nanocomposite powders at different milling times. Comparison between the two used procedures revealed faster particle size refinement in sample A. The average crystallite size of the two samples is not remarkably different but the dehydrogenation

Table 2
Powder characteristics, dehydrogenation temperature (T), and the amount of hydrogen release at 300 °C (H_{300}) and the maximum hydrogen release (H_M) for MgH_2–5 at% ($TiCr_{1.2}Fe_{0.6}$) nanocomposite prepared by two procedures of using elemental Ti–Cr–Fe powder mixture (A) and prealloyed Ti-based BBC alloy (B) at some selected milling times. d and ε show the average crystallite size and lattice strain of β-MgH_2 phase, respectively.

System	Time (h)	D_{50} (nm)	d (nm)	ε (%)	T (°C)	H_{300} (wt%)
A	2	218	20	0.4	288	2.0
	4	185	9	0.9	262	4.9
	6	88	18	0.5	353	2.7
B	2	242	24	0.2	281	2.8
	4	189	7	0.7	241	5.1
	6	150	20	0.3	301	3.1

temperature of sample A and the amount of hydrogen release are slightly higher than the other. To compare the dehydrogenation behavior of the specimens, a STA (DTA-TG) test was performed. Fig. 3 shows the dehydrogenation of the composite materials as a function of temperature for the materials milled for 2 h and 4 h. It is worth mentioning that mechanical alloying for 6 h did not yield a high H-kinetics (see the supplementary document) alike to magnesium hydride powder [13]; hence, the data were not included in

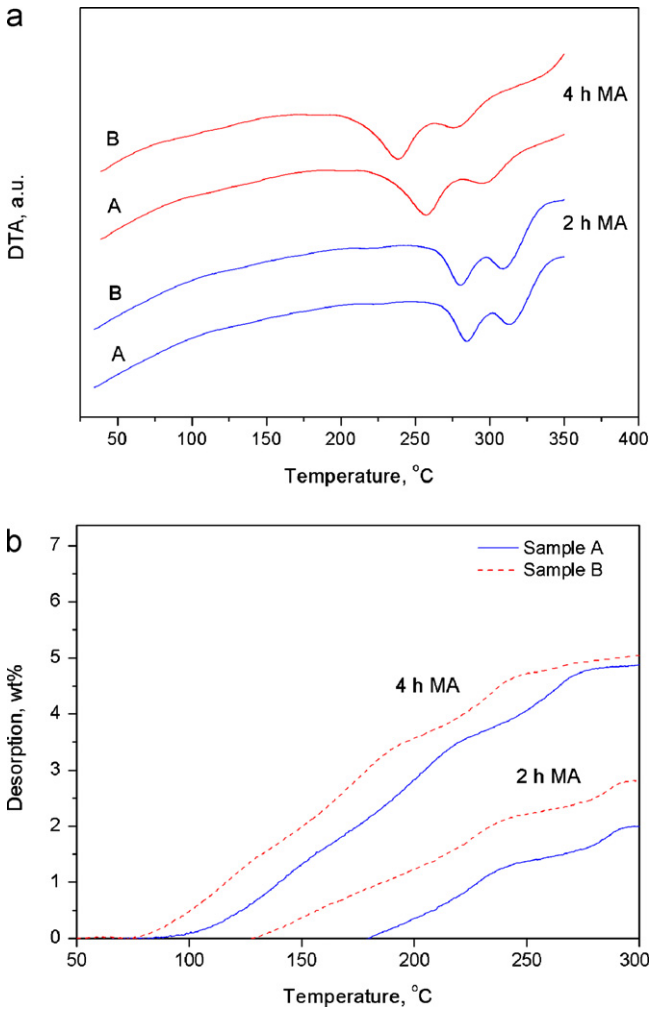

Fig. 3. Effect of Ti-based bcc alloy on the dehydrogenation of nanostructured MgH_2 at some selected milling times. The straight solid lines show the dehydrogenation of composite material obtained by co-milling of MgH_2 and elemental powders of the transition metals (sample A) while the dash lines correspond to the composite material obtained co-milling of MgH_2 and prealloyed $TiCr_{1.2}Fe_{0.6}$ alloy (sample B).

the graph. Each DTA curve (Fig. 3a) contains two distinct endothermic peaks, which correspond to the hydrogen release reaction. The position of the first peak indicates the temperature at which the dehydrogenation reaction has the maximum rate (more endothermic) and thus it is considered as the dehydrogenation temperature in this work. An improvement in the dehydrogenation was achieved by increasing the MA time from 2 h to 4 h. The data presented in Table 2 reveal that as compared to the mechanically activated MgH_2, significant reduction in the dehydrogenation temperature from 327 °C to 262 °C (for sample A) and 241 °C (for sample B) was attained via co-milling with the Ti-based alloy. Nevertheless, the maximum amount of desorption (~5.5 wt%) was lower than pure magnesium hydride due to the addition of Ti-base alloy and the oxidation of the magnesium hydride during mechanical alloying.

4. Discussion

The experiment results showed that combined effects of Ti, Cr, and Fe additives are favorable with respect to the improvement of the dehydrogenation characteristics of MgH_2. Four different reasons are identified to explain this behavior as discussed below.

4.1. Effect of particle size

The results presented in Tables 1 and 2 reveal that the Ti–Cr–Fe additive either in the form of elemental powders (sample A) or prealloyed powder (sample B) accelerates the size reduction of magnesium hydrides during mechanical milling. It is known that MA of magnesium hydride is accompanied by fracturing as well as clustering and cold-welding into larger particles; hence, very fine particles cannot be achieved at the selected milling times as shown in reference [13]. It is suggestible that the addition of relatively ductile Ti–Cr–Fe powders acted as a process control agent during mechanical alloying, inhibiting the micro-welding of the magnesium hydride particles. This effect has also been observed by other researchers for brittle–ductile systems [6–9,12,18]. The differences between the elemental powders with that of prealloyed particles obtained by mechanical alloying could be related to wide differences in the particle size of the metal catalysts (100–150 μm for sample A and 0.38 μm for sample B) as well as the chemical and mechanical nature of the alloys and transient metals. Varin and Czujko [33] reported a profound effect of particle size on the decomposition temperature of MgH_2 after a certain critical threshold value (~2 μm). The mean particle size of MgH_2–5 at% ($TiCr_{1.2}Fe_{0.6}$) nanocomposite ranges between 88 nm and 242 nm which is substantially lower than that of magnesium hydride milled for an equal time (27–51 μm). The finer particles exhibits faster dehydrogenation kinetics due to higher surface area and shorter diffusion distances.

4.2. The role of grain structure

It was shown that finer grain structure is achieved when MgH_2 powder is co-milled with the Ti-based bcc alloy. For instance after 4 h MA, the crystallite size of the nanocomposites is almost one-third of pure magnesium hydride (7 nm versus 25 nm; see Tables 1 and 2). Since the diffusion of H-atoms in grain boundaries is much faster than that of entire lattice and the boundaries are suitable locations for depletion of hydride phase, it is acceptable that finer grain structure promotes the dehydrogenation properties. Here, it should be noted that the lattice strain also affects the H-kinetics significantly [34]. No significant effect of the Ti-based bcc alloy on the accumulated lattice strain of magnesium hydride was noticed, thereby, the effect of lattice strain on the observed results was marginal.

4.3. Formation of binary hydrides

The XRD pattern shown in Fig. 3 revealed the formation of titanium hydride during co-milling of MgH_2 with the Ti-based bcc powder. No metastable ternary Mg–Ti–H phases were formed under the current experimental conditions based on the XRD results, which is in agreement with previous reports [11,12]. Titanium hydride ($\Delta H = -67\ kJ\ mol^{-1}$) is thermodynamically less stable than magnesium hydride ($\Delta H = -75\ kJ\ mol^{-1}$) but the dehydrogenation occurs in two-step processes with high decomposition activation energies [25]. Khrussanova et al. [9] mentioned that at the expense of hydrogen content, Ti 'pump' hydrogen to the magnesium surface and thus catalyze the dehydrogenation process. Very recently, Lu et al. [11] have shown that nanostructured MgH_2–$0.1TiH_2$ prepared by high-energy mechanical alloy exhibits excellent cyclic stability with a high dehydrogenation kinetics. It was suggested that the addition of TiH_2 into MgH_2 changed the reaction thermodynamics of magnesium hydride by weakening the Mg–H bond in consistent with theoretical predictions of the reaction enthalpy performed by Song et al. [35]. Nanostructured titanium hydride could also act as active catalytic sites for adsorption and dissociation of hydrogen which improves the dehydrogenation kinetics of magnesium [11]. On the other hand, the high-pressure orthorhombic γ-MgH_2 phase was formed through localized on-contact impacting action of the milling balls on the low temperature tetragonal β-phase. The metastable phase, which has a lower desorption enthalpy and temperature [36], would affect the thermodynamics and kinetics of dehydrogenation process. Based on the XRD peak intensity ratio of β to γ-phase, one may consider the presence of higher amounts of the metastable phase in the nanocomposites compared to pure magnesium hydride. This implies another factor on the source of different dehydrogenation response of the powders.

4.4. Effect on active surface sites

It is known that iron and chromium do not form binary hydrides but play the role of active sites on the surface of the magnesium particles thus ease the dissociative chemiosorption of hydrogen [9]. In fact, the transition metals chemiosorb hydrogen and transfer hydrogen to the magnesium matrix. Their interface with magnesium also acts as active sites for nucleation of the hydride phase, thereby decreasing the nucleation barrier. This alters the rate-limiting step from nucleation and growth to phase boundary migration [12]; thus, enhanced dehydrogenation is obtained.

5. Conclusions

Nanostructured MgH_2–5 at% ($TiCr_{1.2}Fe_{0.6}$) composite was prepared by co-milling of MgH_2 with Ti-based alloy. The following conclusions can be summarized.

- High-energy mechanical alloying of the Ti–Cr–Fe powder mixture for 6 h yielded nanostructured bcc phase alloy with an average crystallite size of 14 nm.
- The addition of Ti-based bcc alloy to magnesium hydride and mechanical alloying for 4 h reduced the dehydrogenation temperature of magnesium hydride from 327 °C to 241 °C with a hydrogen release of 4 wt% and, average crystallite size of 7 nm, which was remarkably lower than that of milled MgH_2 powder (25 nm) at the same condition.
- Co-milling of MgH_2 with a powder mixture of Ti, Cr, and Fe resulted in the formation of nanostructured composite material with an average crystallite size of 9 nm. XRD and TEM studies

revealed gradual dissolution of titanium in the bcc phase. The dehydrogenation temperature was measured to be around 262 °C with a hydrogen release of 5.5 wt%.
- Comparison between the addition of Ti-based bcc phase as elemental powder mixture (sample A) and prealloyed powder (sample B) showed an enhanced H-kinetics with regard to the dehydrogenation temperature for the latter material.

Appendix A. Supplementary data

Supplementary data associated with this article can be found, in the online version, at doi:10.1016/j.jpowsour.2011.01.001.

References

[1] G. Sandrock, G. Thomas, Appl. Phys. A 72 (2001) 153–155.
[2] B. Sakintuna, F. Lamari-Darkrim, M. Hirscher, Int. J. Hydrogen Energy 32 (2007) 1121–1140.
[3] M. Bououdina, D. Grant, G. Walker, Int. J. Hydrogen Energy 31 (2006) 177–182.
[4] A. Maddalenaa, M. Petrisa, P. Paladea, S. Sartoria, G. Principia, E. Settimob, B. Molinasc, S.L. Russod, Int. J. Hydrogen Energy 31 (2006) 2097–2103.
[5] T. Konto, Y. Sakurai, J. Alloys Compd. 417 (2006) 164–168.
[6] X. Liu, Z. Huang, L. Liang, S. Wang, Int. J. Hydrogen Energy 32 (2007) 965–968.
[7] K. Asano, H. Enoki, E. Akiba, J. Alloys Compd. 486 (2009) 965–968.
[8] J. Guo, K. Yang, L. Xu, Y. Liu, K. Zhou, Int. J. Hydrogen Energy 32 (2007) 2412–2416.
[9] M. Khrussanova, E. Grigorova, I. Mitov, D. Radev, P. Peshev, J. Alloys Compd. 327 (2001) 230–234.
[10] H. Gu, Y. Zhu, L. Li, Int. J. Hydrogen Energy 33 (2008) 2970–2974.
[11] J. Lu, Y.J. Choi, Z.Z. Fang, H.Y. Sohn, E. Ro¨nnebro, J. Am. Chem. Soc. 131 (2009) 15843–15852.
[12] G. Liang, J. Huot, S. Boily, A. Van Neste, R. Schulz, J. Alloys Compd. 292 (1999) 247–252.
[13] H. Simchi, A. Kaflou, A. Simchi, Int. J. Hydrogen Energy 34 (2009) 7724–7730.
[14] G. Barkhordarian, T. Klassen, R. Bormann, J. Alloys Compd. 364 (2004) 242.
[15] T. Kuji, S. Nakayama, N. Hanzawa, Y. Tabira, J. Alloys Compd. 357 (2003) 356–357.
[16] Y. Zhang, Y. Tsushio, H. Enoki, E. Akiba, J. Alloys Compd. 393 (2005) 147.
[17] Y. Zhang, Y. Tsushio, H. Enoki, E. Akiba, J. Alloys Compd. 393 (2005) 185.
[18] P. Palade, S. Sartori, A. Maddalena, G. Principi, S. Lo Russo, M. Lazarescu, G. Schinteie, V. Kuncser, G. Filoti, J. Alloys Compd. 415 (2006) 170–176.
[19] G. Liang, J. Huot, S. Boily, A. Van Neste, R. Schulz, J. Alloys Compd. 297 (2000) 261–265.
[20] W. Oelerich, T. Klassen, R. Bormann, J. Alloys Compd. 315 (2001) 237.
[21] J. Huot, M.L. Tremblay, R. Schulz, J. Alloys Compd. 603 (2003) 356–357.
[22] S. Dal To'e, S.L. Russo, A. Maddalena, G. Principi, A. Saber, S. Sartori, T. Spataru, Mater. Sci. Eng. 108B (2004) 24.
[23] S.W. Cho, G. Shim, G.S. Choi, C.N. Park, J.H. Yoo, J. Choi, J. Alloys Compd. 430 (2007) 136–141.
[24] B.K. Singh, G. Shim, S.W. Cho, Int. J. Hydrogen Energy 32 (2007) 4961–4965.
[25] V. Bhosle, E.G. Baburaj, M. Miranova, K. Salama, Mater. Sci. Eng. A356 (2003) 190–199.
[26] M. Okada, T. Kuriiwa, T. Tamura, H. Takamura, A. Kamegawa, J. Alloys Compd. 511 (2002) 330–332.
[27] X.B. Yu, Z. Wu, B.J. Xia, N.X. Xu, J. Alloys Compd. 372 (2004) 272–277.
[28] X.B. Yu, Z. Wu, N.X. Xu, J. Phys. B 344 (2004) 456–461.
[29] S.W. Cho, C.S. Han, C.N. Park, E. Akib, J. Alloys Compd. 288 (2009) 294–298.
[30] X.B. Yu, Z. Wu, B.J. Xia, N.X. Xu, J. Alloys Compd. 373 (2004) 134–136.
[31] X.B. Yu, Z.X. Yang, S.L. Feng, Z. Wu, N.X. Xu, Int. J. Hydrogen Energy 31 (2006) 1176–1181.
[32] B. Sakintuna, F. Lamari-Darkrim, B. Dogan, Int. J. Hydrogen Energy 32 (2007) 1121–1140.
[33] R.A. Varin, T. Czujko, Scripta Mater. 46 (2002) 531–535.
[34] H. Simchi, A. Kaflou, A. Simchi, Structural characteristics and desorption properties of nanostructured MgH_2 synthesised by high energy mechanical milling, Powder Metall., in press, DOI: 10.1179/003258909X12502872942372.
[35] Y. Song, Z.X. Guo, R. Yang, Mater. Sci. Eng. 365A (2004) 73.
[36] R.A. Varin, T. Czujko, Z. Wronski, Nanotechnology 17 (2006) 3856–3865.